

Extracting the Landscape and Morphology of Aging Glassy Systems

Paolo Sibani* and Jesper Dall

Fysisk Institut, SDU-Odense Universitet, Campusvej 55, DK-5230 Odense M, Denmark

(Dated: December 2, 2024)

We show how the structure of the energy landscape explored after a quench by an aging glassy system can be extracted from the sequence of barrier and energy ‘records’ collected during a simulation. The approach identifies the landscape structures belonging to the quasi-equilibrium and non-equilibrium regimes, and proposes an operational definition of the widely used concept of a valley. Applying the method to short range Ising spin glasses in two and three dimensions shows that the dynamics is time homogeneous in terms of the transformed time variable $\ln t$ and yields novel information on 1) the size of the rearrangements (‘earthquakes’) leading from one valley to the next and 2) the scaling with size and temperature of the energy barriers and the lowest energy in each valley.

PACS numbers: 02.70.Uu ; 05.40.-a ; 75.50.Lk

Macroscopic properties of thermalizing glassy systems depend on the time (age) elapsed after the quench into the glass phase: on time scales shorter than the age, a state of pseudo thermal equilibrium holds locally within metastable regions of the landscape, while on longer observational time scales the relaxation is manifestly non-stationary [1, 2, 3]. Some models of aging build on heuristic assumptions on the morphology of low energy excitations in real space [4, 5], while others start from a coarse grained state space [6, 7, 8, 9] or, more simply, assume a given distribution of exit times from traps in configuration space [10]. However, two simple and fundamental questions remain unanswered: 1) which dynamical events mark the transition between equilibrium and non-equilibrium dynamics, and 2) how can the *corresponding* structures in configuration and/or real space be identified?

This bears on the issue of complex landscape exploration, a task which has been attacked from many different angles: one possibility [11, 12, 13] is to generate a set of local energy minima and subsequently identify the dynamically important paths among them. Exhaustive exploration [14, 15] and variants hereof [16] give more complete information on the geometry of subsets of states surrounding selected local energy minima. The morphology of low-energy excitations has also been studied for e.g. spin glasses by techniques requiring quenches [17], genetic algorithms [18] and energy minimization of excitations of fixed volume [19, 20]. By way of contrast, the present approach solely relies on the landscape information which can be extracted from the systems own dynamics, i.e. from a time series of energy and barrier values which is collected during the relaxation.

For reasons of space, we will focus on the *non-equilibrium* aging dynamics, leaving a discussion of the fluctuation regime to a forthcoming publication. The variable t will denote the age of the system except when otherwise indicated.

Method: Qualitatively, valleys are sets of configura-

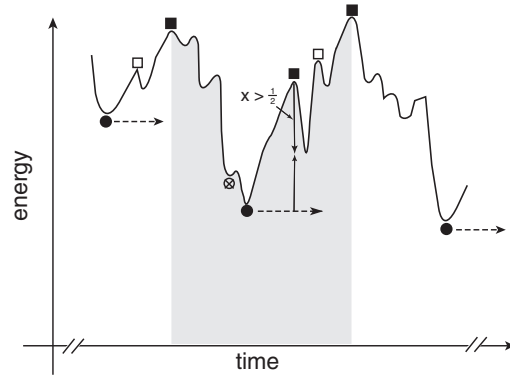


FIG. 1: A fictitious time series of collected energy values illustrates our sampling procedure and our definition of a valley (= gray area). Conspicuous events, i.e. energy and barrier records, are denoted by circles and squares.

tions surrounding local energy minima. Many inequivalent valleys must be present to produce the time inhomogeneous dynamics generally observed in aging systems. Since high-lying and shallow local energy minima are expected to greatly outnumber deep minima, a typical quenched configuration is a poor local minimum and an aging system encounters a series of progressively higher energy barriers [15, 21, 22] which delimit progressively deeper valleys. The values of the highest barrier B and lowest energy E —henceforth *best so far* or simply *bsf* barriers and energies—stand out as crucial events. As explained momentarily, they will serve to identify the valleys as they appear in the energy landscape.

The simulations are performed at a fixed temperature T , starting from a random $T = \infty$ configuration. Barrier values are always computed as energy differences from the current *bsf* energy state. Initially, the *bsf* energy and barrier are set to ∞ and zero, respectively. Each run produces a time ordered sequence of E ’s and B ’s as e.g. *EBBEEBBE* in Fig. 1. Contiguous *bsf* energies pertain to a trajectory ‘tumbling’ down in a valley. Being mainly interested in the configuration where the

tumbling stops, we only keep the lowest E within each group. In Fig. 1 the datum removed is represented by the ‘ \otimes ’ symbol. Similarly, we want to avoid registering the numerous bsf barriers of roughly the same height which appear in close succession while the system goes through a high ‘saddle’. A barrier record is therefore kept only if the energy experiences a sufficiently deep local minimum before the next global barrier maximum is encountered. The precise definition of ‘sufficiently deep’ involves a positive number $x \leq 1$. For $x = 1$, the local minimum must be as low as the current bsf energy, while for $x = 0$ all bsf barriers are kept. Interestingly, our results are insensitive to the value of x in the range $0.25 - 0.75$. In terms of Fig. 1, we only keep the full squares and circles, thereby reducing our string even further to its final state: *EEBEBE*.

For speed we rely on the Waiting Time Method (WTM), a rejection-less Monte Carlo scheme [23] well suited for problems where N variables contribute additively to the energy through local interactions. Based on the local field, each variable is stochastically assigned a *flipping time* and the variable with the shortest flipping time is updated together with the local fields affected by the move. The sequence of moves generated equals in probability [23] the sequence of accepted moves in the conventional Metropolis algorithm, and the current flipping time, henceforth simply ‘time’, closely matches a MC sweep as well as the physical time of an experiment.

The usefulness of our approach rests on the fulfillment of the following conditions: 1) the dynamics is equilibrium-like while the system is confined in a valley, 2) crossing a valley boundary—a barrier event—entails a major reorganization of the configuration, which we refer to as an ‘earthquake’, and 3) the aging behavior of the quantities of interests, e.g. average bsf energy and size of the barriers, is simply parametrized in terms of the valley index. These features are demonstrated in the sequel for spin glass models.

Results: We consider L^d Ising spins placed on a regular lattice of linear size L which interact via the Edwards-Anderson Hamiltonian [24]

$$\mathcal{H}(\alpha) = -\frac{1}{2} \sum_{i,j} J_{ij} s_i^{(\alpha)} s_j^{(\alpha)}. \quad (1)$$

In this formula, $s_i^{(\alpha)}$ is the spin value at site i for configuration α , the couplings J_{ij} are symmetric in their two indices and vanish unless i and j belong to neighbor sites. In the latter case they are drawn independently from a Gaussian distribution of unit variance. The dynamics is nearest neighbor thermal hopping with detailed balance. The runs spanned over several time decades, always bringing the system down to quite low energies, typically around -1.66 per spin. Large systems tend to have more shallow valleys than smaller system. To obtain meaningful comparisons all data originating from the

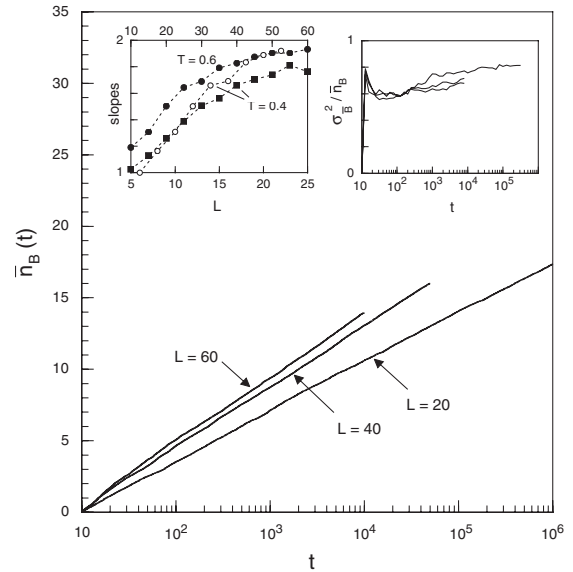


FIG. 2: Main figure: the average number \bar{n}_B of barrier records versus time for three selected system sizes in $2d$ at $T = 0.4$. Left insert: the logarithmic slopes of \bar{n}_B as a function of the linear system size L for $2d$ ($T = 0.4$ and 0.6) and $3d$ ($T = 0.4$). The upper (lower) scale refers to $2d$ ($3d$) systems. Right insert: the variance to average ratio for $n_B(t)$ for the data in the main figure.

first ten time units after the quench were discarded, and the value of the valley index was shifted up to one unit in our scaling plots in Figs. 3 and 4.

A basic quantity is the number of events (barrier or energy records) which on average occur in $[0, t]$. Since achieving a record becomes increasingly difficult, the rate of events will decrease in time and the dynamics decelerates. Interestingly, a time homogeneous dynamics is restored by using the natural logarithm $\ln t$ as time variable. This is shown in Fig. 2, where the average number $\bar{n}_B(t)$ of barrier crossing events is plotted as a function of $\ln t$. The data shown in the main figure belong to $2d$ systems, while similar data in both $2d$ and $3d$ were omitted for clarity. The left insert shows the logarithmic rate of events $d\bar{n}_B(t)/d\ln t$, in $2d$ as well as $3d$, as a function of L . Finally, the right insert shows the ratio of the variance $\sigma_{\bar{n}_B}^2(t)$ to $\bar{n}_B(t)$. Both quantities were estimated for 1000 independent runs: The variance and the average follow the same logarithmic fashion, with the former trailing the latter due to an initial lag.

The approximate equality between average and variance points to an approximate description in term of *log-Poisson* statistics. The name stresses that $\ln t$ rather than t is the relevant time variable, while the statistics describes e.g. the number of magnitude records achieved in a sequence of t independent random numbers [25]. For data stemming from a nearest neighbor random walk in a *landscape*, it indicates a *de-correlation* of the energy function between consecutive barrier records, and *a fortiori* during the time spent within each valley. By identify-

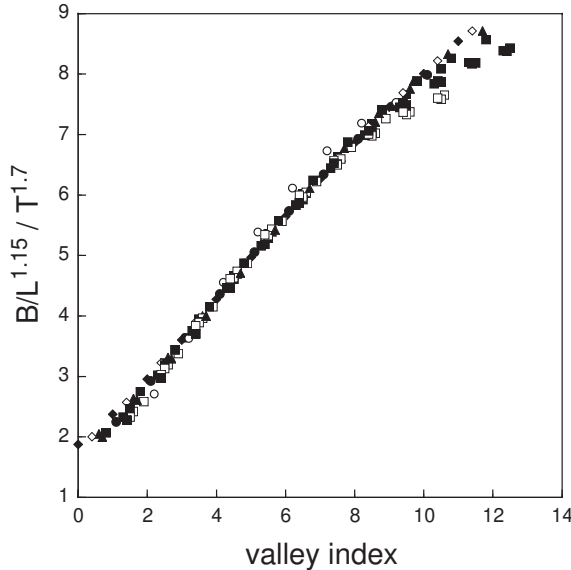


FIG. 3: Energy barriers separating contiguous valleys in 3d scaled with L and T as indicated in the label of the ordinate. Data include $L = 6, 8, 10, 12, 14, 16, 18$ and $T = 0.4, 0.5, 0.6$.

ing the correlation time with the characteristic time for the internal thermalization, we tentatively conclude that thermal quasi-equilibrium is achieved within a valley. As a consequence, the morphology of quasi-equilibrium fluctuations around the bsf state of each valley can be isolated from the non-equilibrium dynamics and analyzed separately.

We now switch to the symbol t_w for the system age and let t be an observational time scale. Consider an arbitrary function F of the number of barrier crossing events, and hence of $\ln(t+t_w)$. A Taylor expansion yields

$$F(\ln(t+t_w)) = F(\ln(t_{max})) + \frac{t_{min}}{t_{max}} F'(\ln(t_{max})), \quad (2)$$

where $t_{max} = \max\{t, t_w\}$ and $t_{min} = \min\{t, t_w\}$. The above t/t_w scaling, well known in spin glass dynamics [26] and from analytical solutions of spin glass models [6, 27], appears in the present context as an immediate consequence of the log-time homogeneity of the dynamics.

The scaling of the logarithmic rate of events with L is shown in the left insert of Fig. 2 to increase from an initial value of 1 to approximately 2 for large system sizes. With Poisson statistics, this rate is proportional to the number of independently evolving lattice ‘regions’. As the spins are quiescent most of the time, a record in any one of these regions leads to an overall record as well. Thus two length scales [20] might in principle coexist in the system: the linear size of the quasi-equilibrium fluctuations and the linear extent of the non-equilibrium ‘earthquakes’ which lead from one valley to the next. However, our data imply that the second length scale is in fact asymptotically equal to L . This is confirmed by the distribution (not shown) of the number of spins having different orientations (i.e. the Hamming distance) in the lowest energy

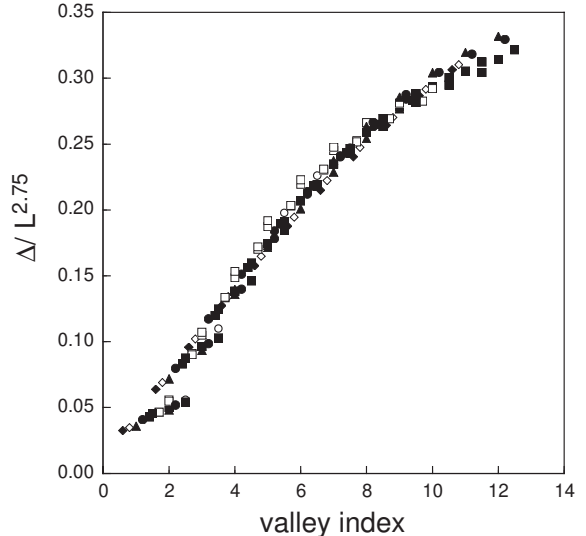


FIG. 4: The difference between the bsf energy of the first and the n 'th valley in 3d is plotted versus n . The energy difference is scaled with L as indicated in the label of the ordinate. Data include $L = 6, 8, 10, 12, 14, 16, 18$ and $T = 0.4, 0.5$ and 0.6 .

configurations of valleys n and $n + 1$. The distribution is found to be exponential, with an average which grows linearly in both n and L^d . The fact that two independent regions can be identified in the system on the time scales investigated might be related to the triviality of the ground states of Gaussian spin glasses [18, 28].

The scaling of energy barriers B separating two contiguous valleys with both L and T in 3d is shown in Fig. 3. All points are quenched averages over 3000 independent runs for $L = 6, 8, 10, 12, 14, 16$ and 18, and with $T = 0.4, 0.5$ and 0.6. As mentioned, the data have been shifted by up to one unit along the abscissa, which mirrors the arbitrariness of the initial bsf states—conventionally recorded after ten time units. As indicated in the plot, $B \propto L^{1.15}T^{1.7}$. We have not attempted a quantitative determination of the uncertainty on the scaling exponents, but changing the last significant digit visibly affects the quality of the plot.

The above considerations apply equally well to Fig. 4, which, for the same set of runs, depicts the average difference $\Delta(1, n)$ between the bsf energy of valley 1 and n . $\Delta(1, n)$ is independent of T , as one should expect, and increases linearly with the valley index. Refs. [7, 9] analyze a mesoscopic model with this exact property. The curvature for large n might partly be due to a systematic error, since not every run enters the last few valleys within the maximum time span allotted to the calculations. For very long time scales, the curve will approach the constant value of the difference between the first bsf energy and the energy of the ground state.

The strong $L^{2.75}$ size dependence of $\Delta(1, n)$ is noticeable: since moving from one valley to the other involves the rearrangements of $\mathcal{O}(L^3)$ spins, it seems likely

that the set difference between two bsf energy configurations be a sponge-like object of the sort discussed in [19, 20]. The energy difference between different bsf states is clearly not $\mathcal{O}(1)$ as expected in a mean-field approach, and it seems unlikely that going to lower energies would radically change the scaling of Δ with system size.

In summary, the method proposed describes an aging process in terms of a set of discrete events which mark the appearance of new valleys in the energy landscape. The homogeneity of the event statistics in the transformed time variable $\ln t$ relates quite simply to the t/t_w scaling of aging data. The logarithmic derivative of the average number of events provides an estimate of the number of regions in real space which can age independently. For spin glasses this number approaches a limit, likely two. Sizes larger than those used in most spin glass studies must be considered in order to reach the asymptotic regime. The scaling of the energies and barriers with L and T suggests that sponge-like objects may describe the (set) difference between very low energy configurations. However, we fail to find any sign of the $\mathcal{O}(1)$ energy differences between low energy states postulated by mean field scenarios of short range models.

Driven dissipative models [25, 29], models of evolution [30, 31, 32] and spin glasses strongly differ at the microscopic level. Yet, their dynamics is homogeneous in $\ln t$ and can be idealized into a log-Poisson process if the ‘events’ marking the transitions from one metastable regime to the next are correctly identified. It thus seems possible to obtain a generic description of aging dynamics.

Acknowledgments: PS is indebted to Greg Kenning and Henrik J. Jensen for discussions and to the Danish SNF for grant 23026.

* Corresponding author paolo@planck.fys.sdu.dk

- [1] M. Alba, M. Ocio, and J. Hammann, *Europhys. Lett.* **2**, 45 (1986).
- [2] P. Svedlindh, P. Granberg, P. Nordblad, L. Lundgren, and H. Chen, *Phys. Rev. B* **35**, 268 (1987).
- [3] J.-O. Andersson, J. Mattsson, and P. Svedlindh, *Phys. Rev. B* **46**, 8297 (1992).
- [4] D. S. Fisher and D. A. Huse, *Phys. Rev. B* **38**, 373 (1988).
- [5] G. Koper and H. Hilhorst, *J. Phys. (Paris)* **49**, 429 (1988).
- [6] P. Sibani and K. H. Hoffmann, *Phys. Rev. Lett.* **63**, 2853 (1989).
- [7] P. Sibani and K. Hoffmann, *Europhys. Lett.* **16**, 423 (1991).
- [8] Y. G. Joh, R. Orbach, and J. Hamman, *Phys. Rev. Lett.* **77**, 4648 (1995).
- [9] K. Hoffmann, S. Schubert, and P. Sibani, *Europhys. Lett.* **38**, 613 (1997).
- [10] J. Bouchaud, *J. Phys. I France* **2**, 1705 (1992).
- [11] F. H. Stillinger and T. A. Weber, *Phys. Rev. A* **28**, 2408 (1983).
- [12] K. Nemoto, *J. Phys. A* **21**, L287 (1988).
- [13] O. M. Becker and M. Karplus, *J. Chem. Phys.* **106**, 1495 (1997).
- [14] P. Sibani, C. Schön, P. Salamon, and J.-O. Andersson, *Europhys. Lett.* **22**, 479 (1993).
- [15] P. Sibani, *Physica A* **258**, 249 (1998).
- [16] J. C. Schön, H. Putz, and M. Jansen, *J. Phys.: Condens. Matter* **8**, 143 (1996).
- [17] J.-O. Andersson and P. Sibani, *Physica A* **229**, 259 (1996).
- [18] M. Palassini and A. P. Young, *Phys. Rev. Lett.* **83**, 5126 (1999).
- [19] J. Houdayer and O. C. Martin, *Europhys. Lett.* **49**(6), 794 (2000).
- [20] J. Lamarcq, J. P. Bouchaud, O. C. Martin, and M. Mezard, *Europhys. Lett.* **58**, 321 (2002).
- [21] Y. G. Joh, R. Orbach, G. G. Wood, J. Hammann, and E. Vincent, *Phys. Rev. Lett.* **82**, 438 (1999).
- [22] M. Lederman, R. Orbach, J. Hammann, M. Ocio, and E. Vincent, *Phys. Rev. B* **44**, 7403 (1991).
- [23] J. Dall and P. Sibani, *Comp. Phys. Comm.* **141**, 260 (2001).
- [24] S. F. Edwards and P. W. Anderson, *J. Phys. F* **5**, 965 (1975).
- [25] P. Sibani and P. B. Littlewood, *Phys. Rev. Lett.* **71**, 1482 (1993).
- [26] J. Kisker, L. Santen, M. Schreckenberg, and H. Rieger, *Phys. Rev. B* **53**, 6418 (1996).
- [27] L. F. Cugliandolo and J. Kurchan, *Phys. Rev. Lett.* **71**, 173 (1993).
- [28] C. M. Newman and D. L. Stein, *Phys. Rev. E* **57**, 1356 (1998).
- [29] P. Sibani and C. M. Andersen, *Phys. Rev. E* **64**, 021103 (2001).
- [30] P. Sibani, M. Brandt, and P. Alstrøm, *Int. J. Modern Phys. B* **12**, 361 (1998).
- [31] P. Sibani and A. Pedersen, *Europhys. Lett.* **48**, 346 (1999).
- [32] M. Hall, K. Christensen, S. A. di Collabiano, and H. J. Jensen, *cond-mat/0202047* (2002).